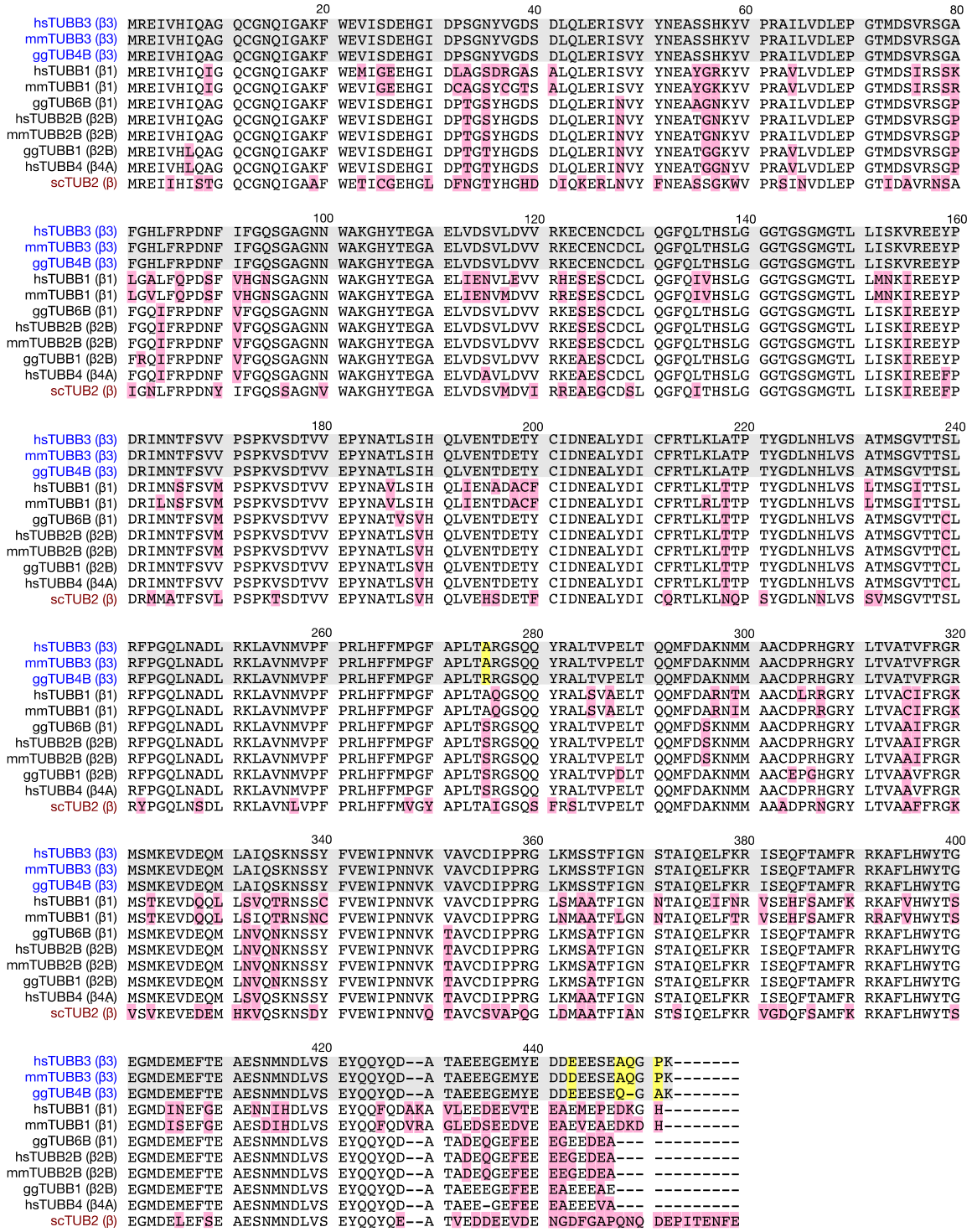

Supplementary Figure 1. Sequence comparison of β-tubulin isotypes in vertebrates and yeast. The sequences of β3 isotypes are highly conserved in vertebrates, showing only three amino acid residue differences between humans and chickens (coloured in yellow). In contrast, the sequence of human β3-tubulin differs from that of human β1, β2B, β4A-tubulin and yeast β-tubulin at 100, 34, 32 and 123 residues, respectively (coloured in pink). For each isotype, the sequence was obtained from UniProt (http://www.uniprot.org/): AAH03021 (human β3, hsTUBB3), AAH88749 (mouse β3, mmTUBB3), AAA49119 (chicken β3, ggTUB4B), AAH33679 (human β1, hsTUBB1), AAI47699 (mouse β1, mmTUBB1), AAA49124 (chicken β1, ggTUB6B), AAH63610 (human β2B, hsTUBB2B), BAE40722 (mouse β2B, mmTUBB2B), CAA23687 (chicken β2B, ggTUBB1), AAH13683 (human β4A, hsTUBB4), DAA12403 (yeast β, scTUB2). Amino acid sequences were aligned by clustalX.

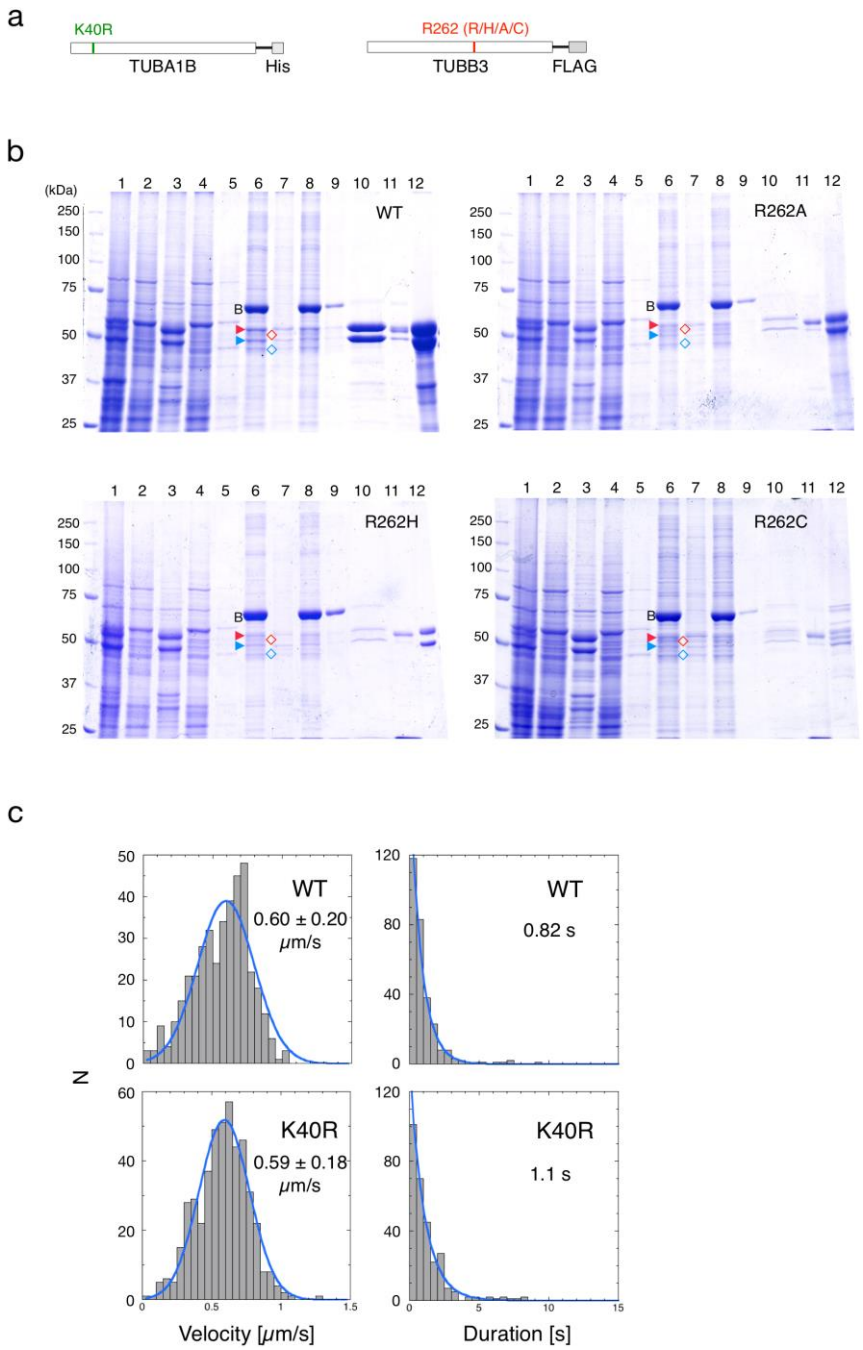

Supplementary Figure 2. Design and preparation of tubulin mutants. (**a**) Design of α- and β-tubulin constructs. These constructs are cloned into a single baculovirus vector. (**b**) SDS PAGE showing each preparation step of WT and R262A, R262H and R262C tubulin. Lanes: (1) Cell lysate, (2) soluble fraction and (3) precipitate after centrifugation, (4) His-affinity column flow-through, (5) His-affinity column wash, (6) His-affinity column eluent (supplemented with 2 mg ml^{-1} BSA), (7) the fraction that remained attached to the His-affinity column, (8) FLAG-affinity column flow-through, (9) FLAG-affinity column wash, (10) FLAG-affinity column eluent, (11) the fraction that remained attached to the FLAG-affinity column, and (12) after polymerization and centrifugation. ▶ and ▶, recombinant α- and β-tubulin; ◇ and ◇, endogenous α- and β-tubulin; B, BSA. (**c**) The effect of residue substitution at α-Lys40 residue on single-molecule motility of KIF5B. To prepare recombinant tubulin with a single post-translational modification state[1], the Lys40 of α-tubulin was substituted by Arg and treated as WT. The velocity and duration of α-K40R MTs was only slightly different from that of inherent WT, in which 10–30 % of α-tubulin is acetylated.

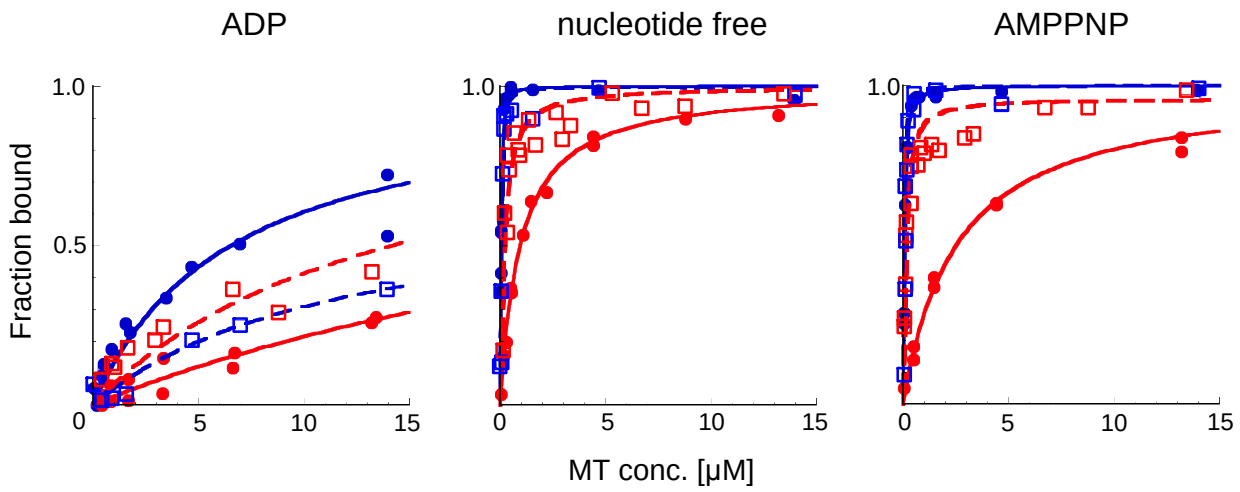

Supplementary Figure 3. Equilibrium dissociation constants of the KIF5B-MT complex. Binding of 0.1 μM single-headed HK349 KIF5B with varying concentrations of MTs. The fraction of HK349 in the MT pellet was plotted as a function of the total MT concentration. ●, WT KIF5B-WT MT; ●, WT KIF5B-R262A MT; □, D279R KIF5B-WT MT; □, D279R KIF5B-R262A MT. For each condition, measurements are repeated 2–3 times and all data from multiple rounds of measurements are plotted in the graph. The curves are the best fit to hyperbola with dissociation constant (K_d) values given in Supplementary Table 2 and Fig. 3f.

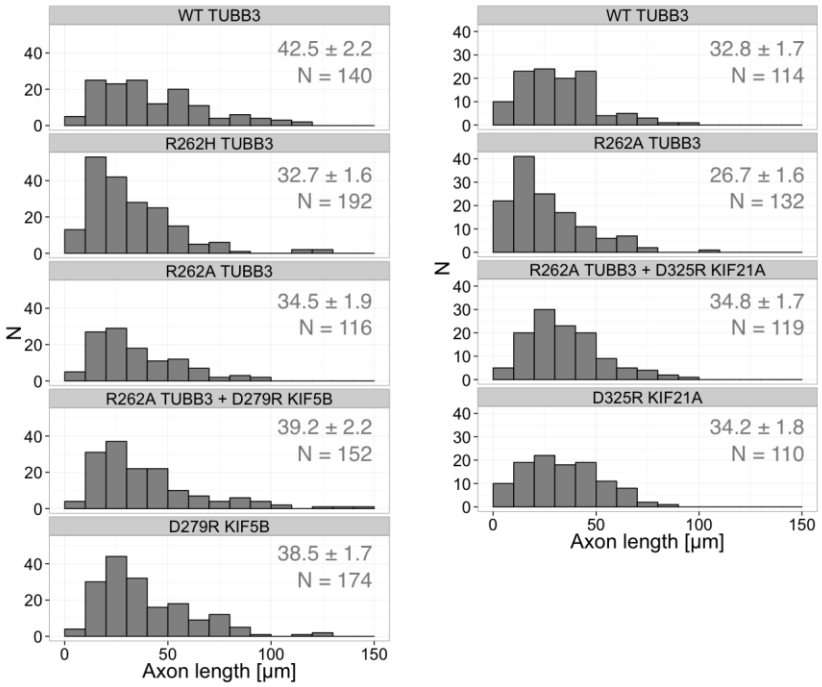

Supplementary Figure 4. Distribution of axon lengths when WT and mutant TUBB3, and/or mutant KIF5B/KIF21A were expressed in mouse cortex neurons. Data from two independent sets of experiment are shown. Numbers indicate mean ± s.e.m. lengths in µm.

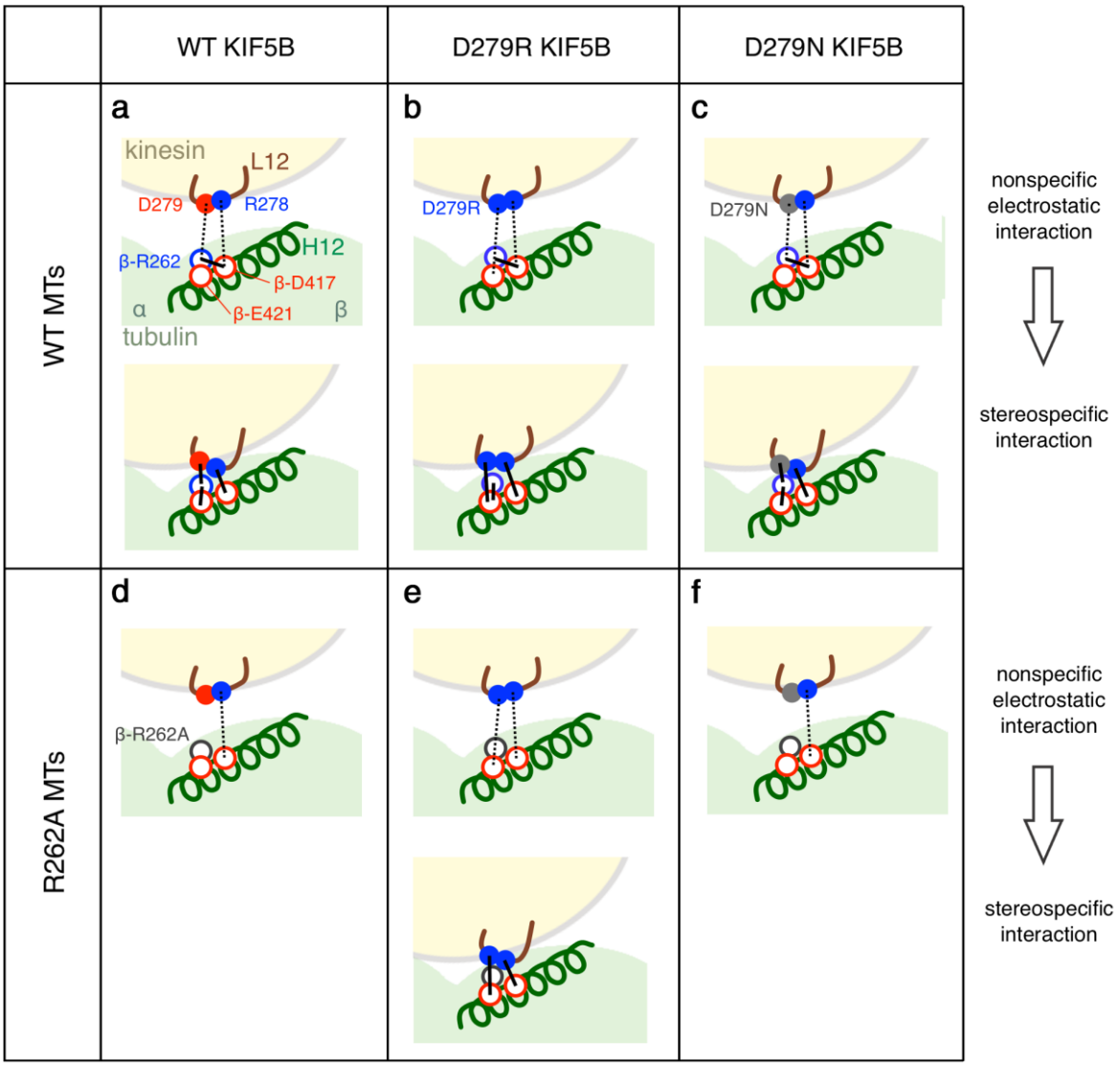

Supplemental Figure 5. Possible models for interactions between the L12 loop in KIF5B and the area near the residue β-R262 in TUBB3. Red, blue, and grey filled circles represent basic, acidic and neutral residues in KIF5B, respectively, whereas red, blue and grey unfilled circles represent basic, acidic and neutral residues in TUBB3, respectively. The dotted line indicates electrostatic attraction. Hydrogen bonds within tubulin molecule (indicated by thick lines) were predicted by using PyMOL, based on the simulated structure of αβ-tubulin dimer with or without β-R262A mutation (PDB: 1JFF)[2].

Both D279R and β-R262A mutations cause breaking of the salt bridge between D279 in KIF5B and R262 in TUBB3, which is formed in a WT-WT pair. However, the effect of each mutation on motility is different: While WT KIF5B was unable to move on β-R262A MT, D279R KIF5B was able to move on WT-MT (Fig. 3c, d, Table 1 in the main text). The result can be explained from the viewpoint of electrostatic interaction. In paired mutant WT KIF5B-β-R262A MT (d), it is difficult for residue D279 to find an alternative binding partner to replace β-R262A, because β-R262 is the only basic residue on an MT within an 8 Å distance from D279 (PDB: 4LNU). On the other hand, in paired mutant D279R KIF5B-WT MT (b), the D279R residue can easily find a binding partner, because the majority of kinesin-interacting tubulin residues are acidic. The local structure of the kinesin-MT interface[3] indicates that the repulsion between D279R and β-R262 could well be compensated for by the salt bridges D279R-β-E421 and R278-β-D417, allowing the pair (D279R KIF5B-WT MT) to stererospecifically bind.

Supplementary Table 1. Comparison of the parameters of microtubule-activated kinesin ATPase in charged-to-alanine tubulin and kinesin mutants

mutant	relative ATPase parameter		protein	reference
	k_{cat} (fold wt)	k_M(MT) (fold wt)		
WT-Tb	1.00 ± 0.03	1.00 ± 0.14	*Homo sapiens* TUBB3	This study[a]
β-Tb R262H	0.17 ± 0.03	9.71 ± 4.94		
β-Tb R262A	0.23 ± 0.01	10.3 ± 1.23		
WT-Tb	1.00 ± 0.03	1.00 ± 0.30	*S. cerevisiae* TUB2	Uchimura, et al, 2010[b]
α-Tb E414A	0.20 ± 0.02	0.78 ± 0.04		
α-Tb E415A	0.80 ± 0.09	2.39 ± 0.22		
α-Tb E417A	0.82 ± 0.03	1.00 ± 0.35		
α-Tb E420A	0.94 ± 0.03	1.83 ± 0.39		
β-Tb E410A	1.21 ± 0.11	6.39 ± 1.70		
β-Tb D417A	1.18 ± 0.05	5.96 ± 0.87		
kinesin R278A	0.66 ± 0.30	15.5 ± 5.45	*Homo sapiens* KIF5B	Woehlke, et al, 1997[c]
kinesin D279A	0.78 ± 0.14	0.44 ± 0.21		

[a] Values are mean ± errors of curve fitting

[b] Values are mean ± s.d. of 4–6 independent measurements[4]

[c] Values are mean ± s.d. of 2–5 independent measurements[5]

Supplementary Table 2. Equilibrium dissociation constants of the KIF5B-MT complex

microtubule	WT KIF5B			D279R KIF5B		
	ADP	nucleotide free	AMPPNP	ADP	nucleotide free	AMPPNP
WT	6.5 ± 0.7	$1.2 \pm 0.6 \times 10^{-2}$	$2.9 \pm 0.4 \times 10^{-2}$	$1.2 \pm 0.8 \times 10^{1}$	$1.2 \pm 0.6 \times 10^{-2}$	$1.0 \pm 0.4 \times 10^{-2}$
β-R262A	$3.6 \pm 0.3 \times 10^{1}$	$8.6 \pm 0.4 \times 10^{-1}$	2.5 ± 0.1	$1.4 \pm 0.2 \times 10^{1}$	$1.2 \pm 0.3 \times 10^{-1}$	$5.0 \pm 1.2 \times 10^{-2}$

Values are K_d in μM. Errors are those in curve fitting.

Supplementary Table 3. Summary of single-molecule motility assay of KIF21A on TUBB3 microtubules

microtubule	parameter	KIF21A	
		WT	D325R
WT	velocity [μm s^{-1}]	0.18 ± 0.32	0.24 ± 0.45
	duration [s]	7.70 ± 1.50	6.01 ± 1.74
	run length [μm]	1.56 ± 0.33	1.42 ± 0.41
β-R262H	velocity [μm s^{-1}]	UD	UD
	duration [s]	UD	UD
	run length [μm]	UD	UD
β-R262A	velocity [μm s^{-1}]	UD	0.16 ± 0.45
	duration [s]	UD	5.88 ± 0.89
	run length [μm]	UD	1.61 ± 0.73

Velocities, durations, and run lengths of the values in four independent experiments (N > 60 each, total N > 240; mean ± s.d.). UD, undetected. Motility was measured using BG-549 labeled dimeric construct of KIF21A (KIF21A-552). Only the population of KIF21A molecules showing directional movements was analyzed.

Supplementary References

1. Minoura, I., *et al.* Overexpression, purification, and functional analysis of recombinant human tubulin dimer. *FEBS Lett.* **587**, 3450-3455 (2013).
2. Fiser, A. & Sali, A. ModLoop: automated modeling of loops in protein structures. *Bioinformatics* **19**, 2500-2501 (2003).
3. Cao, L., Wang, W., Jiang, Q., Wang, C., Knossow, M. & Gigant, B. The structure of apo-kinesin bound to tubulin links the nucleotide cycle to movement. *Nat. Commun.* **5**, 5364 (2014).
4. Uchimura, S., Oguchi, Y., Hachikubo, Y., Ishiwata, S. & Muto, E. Key residues on microtubule responsible for activation of kinesin ATPase. *EMBO J.* **29**, 1167-1175 (2010).
5. Woehlke, G., Ruby, A. K., Hart, C. L., Ly, B., Hom-Booher, N. & Vale, R. D. Microtubule interaction site of the kinesin motor. *Cell* **90**, 207-216 (1997).